The EMBO Journal (2005) 24, 170–179 | © 2005 European Molecular Biology Organization | All Rights Reserved 0261-4189/05
www.embojournal.org

THE
EMBO
JOURNAL

5-Lipoxygenase regulates senescence-like growth arrest by promoting ROS-dependent p53 activation

Alfonso Catalano[1,2,*], Sabrina Rodilossi[1], Paola Caprari[1,3], Vincenzo Coppola[3] and Antonio Procopio[1,2]

[1]Department of Molecular Pathology and Innovative Therapies, Polytechnic University of Marche, Ancona, Italy, [2]Laboratory of Cytology, Italian National Research Centers on Aging, Ancona, Italy and [3]Neural Development Group, Mouse Cancer Genetics Program, National Cancer Institute, Frederick, MD, USA

5-Lipoxygenase (5LO) is involved in the production of leukotrienes and reactive oxygen species (ROS) from arachidonic acid. Its strong activation has been associated with several diseases like cancer and neurodegeneration. Here we show that 5LO activity increases during senescence-like growth arrest induced by oncogenic *ras* or culture history in both human and mouse embryo fibroblasts. Overexpression of 5LO promotes senescence-like growth arrest via a p53/p21-dependent pathway, and this occurs independently of telomerase activity. 5LO stabilizes p53 through phosphorylation at Ser15 and increases expression of the p53-transcriptional target p21. This is achieved by regulating ROS production. Indeed, ROS are increased in 5LO-arrested cells. Antioxidants and a low oxygen environment prevent 5LO-induced growth arrest. Finally, 5LO inhibition reduces the growth arrest induced by oncogenic *ras* or culture history and these effects are neutralized by the addition of exogenous ROS. These data link the 5LO pathway to oxidative crises of primary fibroblast and suggest that the ability of 5LO to induce senescence-like growth arrest may be important in the pathogenesis of 5LO-associated disorders.

The EMBO Journal (2005) **24,** 170–179. doi:10.1038/sj.emboj.7600502; Published online 16 December 2004
Subject Categories: cell cycle; molecular biology of disease
Keywords: 5-lipoxygenase; oncogenic *ras*; p53; reactive oxygen species; senescence

Introduction

Replicative senescence limits the proliferation of many mammalian cells both *in vitro* and *in vivo* (Campisi, 2001). In human cells, this appears to be primarily mediated by telomere shortening (Stewart and Weinberg, 2000; Mathon and Lloyd, 2001). In addition, oncogene activation, such as the one elicited by activated Ras, and DNA damage induce a premature form of senescence (here reported as 'stasis') irrespective of telomere length (Bringold and Serrano, 2000; Drayton and Peters, 2002). Cellular senescence (replicative senescence and stasis) is considered to be a cellular safeguard mechanism against uncontrolled proliferation and formation of cancer (Campisi, 2001).

Stasis induced by oncogenic *ras* and replicative senescence downstream of telomere shortening share common signaling pathways and morphological features (Lundberg *et al*, 2000; Schmitt, 2003). Typical phenotypic markers are enlarged and flattened morphology, and the β-galactosidase (SA-β-gal) activity. At the molecular level, senescence cells accumulate cell cycle inhibitors, such as p53, $p21^{Cip1/Waf1}$ (p21) and $p16^{INK4a}$ (p16), irreversibly halt in the G1 phase of the cell cycle and fail to phosphorylate retinoblastoma (pRb) after mitogen stimulation (Serrano and Blasco, 2001). Another stress condition that has been linked to the activation of cellular senescence includes oxidative stress and reactive oxygen species (ROS) production. ROS and hydrogen peroxide, in particular, are involved in the induction of stasis by oncogenic *ras* (Lee *et al*, 1999). In human lung fibroblasts, oxidative stress can cooperate with telomere shortening to activate replicative senescence (Atamna *et al*, 2000; Forsyth *et al*, 2003). Moreover, in mouse embryonic fibroblasts (MEFs), oxidative stress appears to be the major mechanism for inducing replicative senescence (Parrinello *et al*, 2003). Although oxidative stress is a feature of cellular senescence, the sources of ROS during replicative senescence and stasis remain elusive.

Increased production of ROS may derive from the NADPH oxidase and from the mitochondria (Haendeler *et al*, 2004). However, there are other sources of cellular ROS, including 5-lipoxygenase (5LO), which is known to catalyze the production of leukotrienes (LTs) and ROS from arachidonic acid (Lewis *et al*, 1990; Soberman and Christmas, 2003). The activity of 5LO is required for ROS production by CD28 stimulation in T lymphocytes (Los *et al*, 1995) and products of 5LO cascade, LTB4 in particular, play roles in the TNF-α-induced production of ROS (Woo *et al*, 2000).

High levels of 5LO and its metabolites are found in a wide variety of human cancers (Soberman and Christmas, 2003). Moreover, we and others have shown that 5LO pathway promotes cancer cell proliferation and survival (Hong *et al*, 1999; Catalano *et al*, 2004). Although these reports suggested an important role of 5LO in human malignancy, the impact of 5LO activation on the growth and lifespan of normal (untransformed) cells is poorly investigated. Here we identified the 5LO pathway as a key signaling involved in oncogenic *ras*-induced stasis and oxidative crises during culture history, and provide evidence that 5LO-linked cascade controls senescence-like growth arrest, in part, by modulating ROS levels and p53 activity.

*Corresponding author. Dipartimento di Patologia Molecolare e Terapie Innovative, Università Politecnica delle Marche, Via Ranieri, 60131, Ancona, Italy. Tel.: +39 07 12 20 46 23; Fax: +39 07 12 20 46 18; E-mail: catgfp@yahoo.it

Received: 21 July 2004; accepted: 11 November 2004; published online: 16 December 2004

Results

5LO expression and activity in oncogenic ras-mediated stasis

We first examined the expression and activity of 5LO during stasis induced by oncogenic *ras* (Ha-RasV12) or sublethal doses of H_2O_2. As previously described, human (WI38, IMR-90 and LF1) and MEFs expressing Ha-RasV12 or treated with H_2O_2 (250 μM for 2 h) reduced [^{3}H]thymidine uptake at subconfluent density (up to 85%) and were highly positive (up to 75%) for senescence-associated SA-β-gal by 10–15 days post-treatments (data not shown; Bischof *et al*, 2002; Gorbunova *et al*, 2002). Unlike H_2O_2, Ha-RasV12-arrested WI38 cells displayed a strong induction in 5LO, and in the senescence-related markers p53 and p21 (Figure 1A). IMR-90, LF1 and MEFs that underwent 'static' by oncogenic *ras* also accumulated 5LO (Figure 1B). These changes were accompanied by a progressive increase in 5LO nuclear localization (data not shown). Accordingly, products of the 5LO pathway, 5-HETE and LTB4, were increased in conditioned media of Ha-RasV12-expressing fibroblasts by four- and three-fold, respectively. The production of the 'total LTA4-derived metabolites' (the sum of LTB4, 20-OH-LTB4, Δ6-*trans*-LTB4 and 12-epi-Δ6-*trans*-LTB4) was also increased by 3.5-fold (Figure 1C). However, Ha-RasV12-arrested cells did not show appreciable changes in 12-HETE, a 12-LO metabolite, or cyclooxygenase (COX) metabolites, compared with control cells (data not shown). Ha-RasV12 upregulated two gene products of the 5LO cascade, cytosolic phospholipase A2 (cPLA2) and 5LO. In addition, oncogenic *ras* gave a 3.5-fold increase in COX2 mRNA, whereas it did not induce a significant change in LTA4 hydrolase, LTC4 synthase and 5LO activating protein (FLAP) mRNA levels (Supplementary Figure 1). H_2O_2 had no appreciable effect on 5LO pathway constituents. It therefore appears that the 5LO cascade is part of the signaling pathway of oncogenic *ras*-induced stasis.

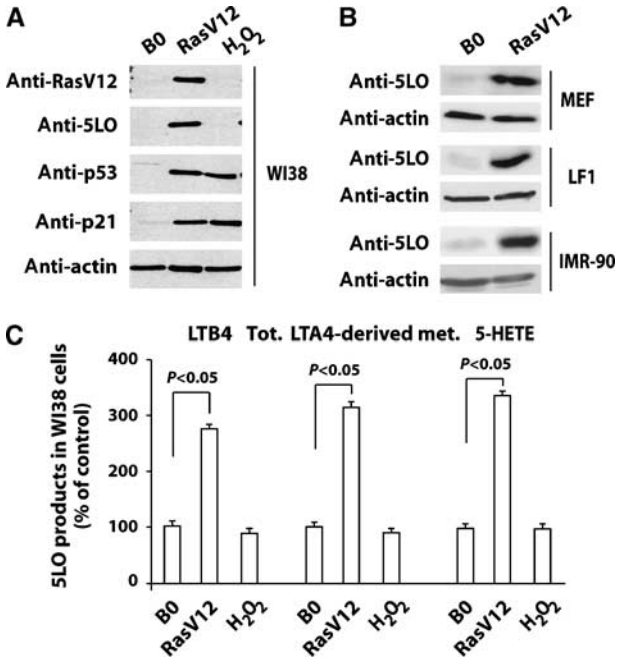

Figure 1 Oncogenic *ras* induces 5LO expression and activity. (**A**) WI38 fibroblasts were infected with empty virus as a control (B0) or Ha-RasV12-expressing retrovirus, or treated with 250 μM H_2O_2 for 2 h. Day 0 is the first day after selection for 4 days in 1 μg/ml puromycin. After 7 days, cells reduced [^{3}H]thymidine uptake and were positive for SA-β-gal activity (data not shown). Cell lysates were then prepared and Western blot analyses of RasV12, 5LO and the senescence-related proteins p53 and p21 were performed. (**B**) Western blot analysis of 5LO in the indicated cells treated as described in the legend to panel A. Expression of actin was used as an internal control. (**C**) Ha-RasV12-infected or H_2O_2-treated WI38 cells were incubated with 10 μM calcium ionophore A23187. After 15 min at 37°C, the reaction was terminated, and the formation of AA metabolites (LTB4, 'total LTA4-derived metabolites' and 5-HETE) was assayed as described in Materials and methods. *P*-values are also indicated, ANOVA, $n = 4$.

5LO is critical for the ROS production and stasis induced by oncogenic ras

ROS production mediates Ha-RasV12-induced stasis (Lee *et al*, 1999). To determine whether 5LO pathway is involved in ROS generation and stasis induced by oncogenic *ras*, Ha-RasV12-arrested WI38 cells were preincubated with the 5LO inhibitors AA861, eicosatetraynoic acid (ETYA) and MK886, and the cPLA2 inhibitor arachidonyl trifluoromethyl ketone (ATK). For comparison purpose, we also used the nonspecific COX inhibitor indomethacin as well as *N*-acetylcysteine (NAC), a ROS scavenger, and diphenyleneiodonium chloride (DPI), an inhibitor of NADPH oxidase-like flavoenzymes, which are known to inhibit stasis (Lee *et al*, 1999; Haendeler *et al*, 2004). AA861 (1 μM) and MK886 (1 μM) potently suppressed (up to 70%) 5-HETE formation in Ha-RasV12-stimulated WI38 cells. ATK (10 μM) also reduced by 60% the amount of 5-HETE, and high concentrations of ETYA (35 μM) were required for similar inhibition (Supplementary Figure 2A). The concentration of these inhibitors corresponded to approximately twice the previously determined ID_{50}. As expected, Ha-RasV12-induced 5LO activity was not significantly affected by indomethacin (10 μM), NAC (2 mM) and DPI (15 μM) (Supplementary Figure 2A). We observed similar findings when LTB4 determination was used instead of 5-HETE (data not shown). Under these conditions, the cPLA2 and 5LO inhibitors markedly decreased Ha-RasV12-induced ROS and SA-β-gal accumulation. By contrast, indomethacin had little or no effect (Supplementary Figure 2B). As expected, NAC and DPI diminished ROS and SA-β-gal accumulation elicited by oncogenic *ras* (Supplementary Figure 2B), whereas AA861, ETYA, MK886 and ATK did not influence ROS and SA-β-gal accumulation after H_2O_2 treatment (data not shown). This suggests that cPLA2-catalyzed synthesis of arachidonic acid and subsequent metabolism of arachidonic acid by 5LO are involved in the Ha-RasV12 signaling to ROS generation and stasis.

To test this idea, Ha-RasV12-induced stasis was analyzed in 5LO-deficient ($5LO^{-/-}$) MEFs. Ha-RasV12-infected wild-type MEFs ceased to proliferate at subconfluent density, whereas Ha-RasV12 expression had a minor and delayed effect on proliferation of $5LO^{-/-}$ MEFs (Figure 2A). The frequency of SA-β-gal-positive cells (data not shown) and DCF fluorescence (Figure 2B, left panel) were significantly lower in oncogenic *ras*-expressing $5LO^{-/-}$ MEFs than in wild-type MEFs. Similar results were obtained when the formation of superoxide anion (O_2^-) was determined by measuring the chemiluminescence of the metabolized lucigenin. In fact, Ha-RasV12 expression in wild-type MEFs resulted in an 8.5-fold increase in O_2^- formation compared to control cells,

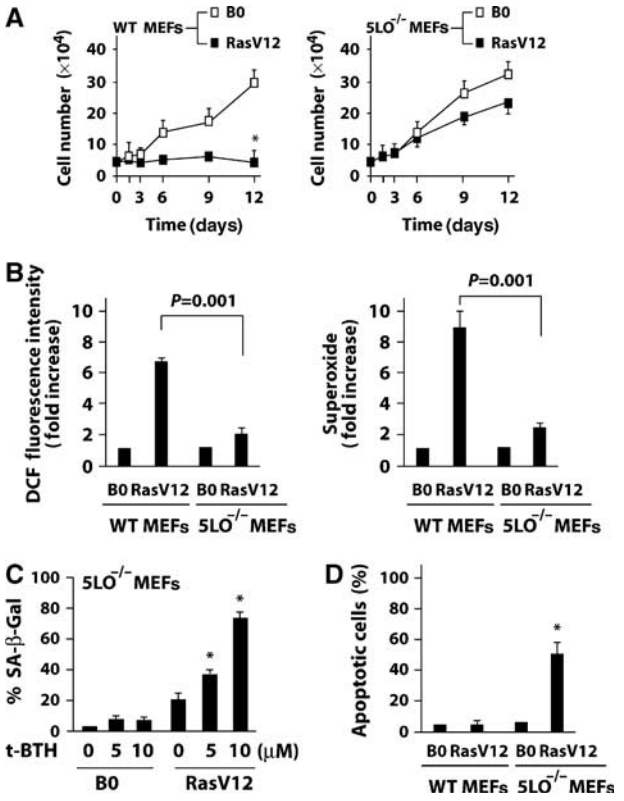

Figure 2 5LO deficiency abolishes oncogenic *ras*-induced ROS production and stasis of MEFs. (**A**) Growth curves of wild-type or $5LO^{-/-}$ MEFs infected with control (B0) or Ha-RasV12 vectors. (**B**) DCF fluorescence intensity (left) and O_2^- recognition by lucigenin (right), assayed as described in Materials and methods, were used as indicators of ROS levels in both wild-type and $5LO^{-/-}$ MEFs infected with B0 or oncogenic *ras*. (**C**) $5LO^{-/-}$ MEFs infected with B0 or oncogenic *ras* were treated with 5 or 10 μM t-BTH for 2 days, that is, from 4 to 6 days after selection. SA-β-gal-stained cells were counted 7 days after selection. (**D**) Annexin–propidium iodide (PI) staining of B0- and Ha-RasV12-infected wild-type or $5LO^{-/-}$ MEFs. $^*P \leqslant 0.05$ versus control, ANOVA, $n = 3$.

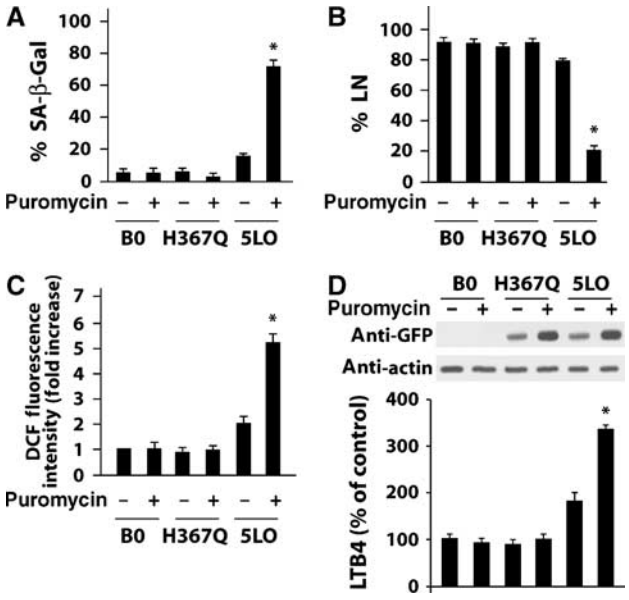

Figure 3 Comparison of the effects of different 5LO protein levels on ROS production and stasis in WI38 cells. (**A, B**) WI38 cells were infected with a pBabe-based vector containing empty (B0), GFP-tagged 5LO or its catalytically inactive mutant (H367Q). Infected cells were then selected or unselected with puromycin (for 4 days, 1 μg/ml). After 7 days, [^{3}H]thymidine was added for 3 days and cells were subsequently stained for SA-β-gal (A) followed by autoradiography (B) as described in Materials and methods. About 500 cells were counted to determine the percentages of radiolabeled nuclei (% LN) and positive SA-β-gal cells (blue). A cell was only considered SA-β-gal positive when it was not radiolabeled. (**C**) ROS detection by DCF fluorescence intensity in WI38 cells after infection with GFP-tagged 5LO or H367Q in the presence or absence of puromycin. (**D**) Conditioned media and protein samples of equal size were then assayed for LTB4 formation (by HPLC procedures) and for 5LO protein expression using an anti-GFP as antibody (inset), respectively. $^*P \leqslant 0.001$ versus B0, ANOVA, $n = 3$.

whereas it caused only a two-fold increase in $5LO^{-/-}$ MEFs (Figure 2B, right panel). The addition of pro-oxidant tert-butyl-H_2O_2 (t-BTH) rescued the antistatic effect in Ha-RasV12-infected $5LO^{-/-}$ MEFs (Figure 2C). Thus, exogenous ROS can cooperate with Ha-RasV12 to overcome the antistatic effect of 5LO deficiency. Extension of lifespan after oncogenic *ras* transduction into $5LO^{-/-}$ MEFs was followed at later passages (at day 12 until day 16) by apoptosis of a large fraction of Ha-RasV12-overexpressing $5LO^{-/-}$ MEFs (Figure 2D). Therefore, oncogenic *ras* may promote either stasis or apoptosis depending on the expression levels of 5LO in the cell.

5LO pathway induces telomerase-independent stasis by increasing intracellular ROS

To further evaluate the role of 5LO pathway in stasis, we introduced a green fluorescent protein (GFP)-tagged 5LO or catalytically inactive 5LO mutant (H367Q) into WI38 fibroblasts using a pBabe-based vector. When WI38 fibroblasts were not selected with puromycin following 5LO infection, 5LO did not induce significant SA-β-gal accumulation and growth arrest. In contrast, after selection, 5LO caused stasis within 10-15 days from infection (Figure 3A and B). ROS levels induced by 5LO, without selection, increased around two-fold over controls, whereas WI38 fibroblasts selected following 5LO infection had a greater than five-fold increase in ROS levels (Figure 3C). These different cell responses were linked with the increased 5LO protein and LTB4 formation observed (Figure 3D). We observed similar results when 5-HETE determination was used instead of LTB4 (data not shown). Notably, overexpression of H367Q was completely ineffective. Thus, quantitative differences in 5LO expression and activity correlated with ROS induction and stasis. Neither cPLA2 nor COX2 overexpression provoked SA-β-gal activity and reduction of [^{3}H]thymidine incorporation, although these proteins were efficiently expressed (data not shown).

To determine what ROS are actually formed in 5LO-expressing cells, we assessed the levels of O_2^-, H_2O_2, NO_2^- and lipid peroxidation. Like oncogenic *ras*, 5LO expression resulted in a nine-fold increase in both O_2^- and H_2O_2 formation compared to H367Q or control cells. Moreover, 5LO as well as Ha-RasV12 caused a four- and three-fold elevation in the level of NO_2^- and lipid peroxides, respectively (Figure 4A). Interestingly, COX2 overexpression also increased lipid peroxidation and NO_2^- formation; however, no generation of oxygen radicals (O_2^- and H_2O_2) has been detected (data not shown).

To better understand the importance of the rise in ROS levels (O_2^- and H_2O_2, mainly) in the development of the

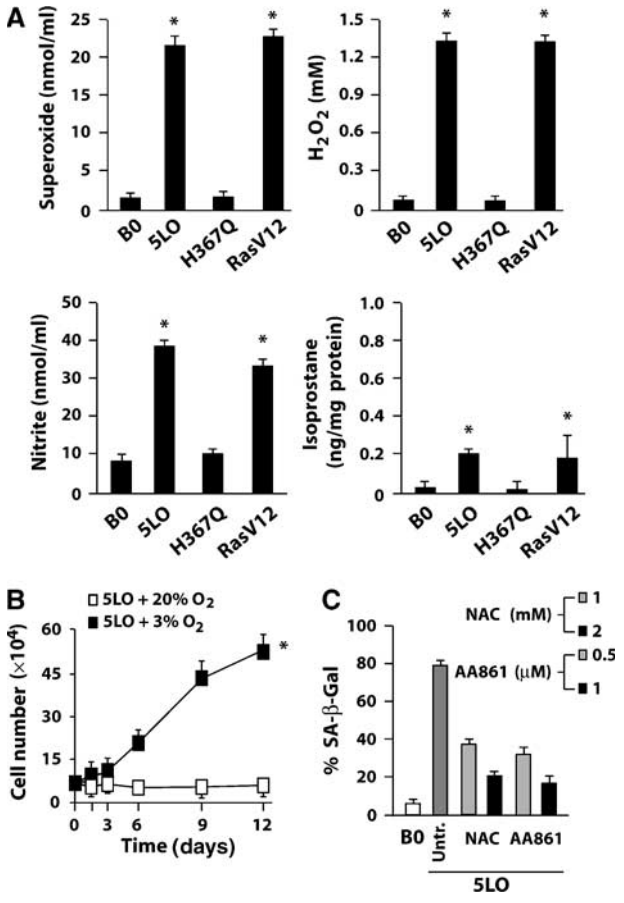

Figure 4 Impact of ROS in 5LO-induced stasis. (**A**) O_2^-, H_2O_2, NO_2^- and 8-isoprostane productions, analyzed as described in Materials and methods, were detected in WI38 cells containing an empty vector (B0), wild-type 5LO, its catalytically inactive mutant (H367Q) or oncogenic *ras*. $^*P \leqslant 0.05$ versus control vector (B0), ANOVA, $n = 3$. (**B, C**) Growth curves and SA-β-gal activity of WI38 fibroblasts infected with the indicated retroviruses. Infected cells were cultured in 20 or 3% oxygen for the indicated period of time (B) or with 1 or 2 mM NAC as well as 0.5 or 1 μM AA861 for 10 days (C). $^*P \leqslant 0.05$ versus cells infected with 5LO in 20% oxygen, ANOVA, $n = 3$.

5LO-induced stasis, we cultured 5LO-expressing cells in varying oxygen environments, an established method to regulate ROS production (Parrinello *et al*, 2003). 5LO-expressing cells maintained in the standard tissue culture environment of 20% oxygen undergo near complete growth arrest. By contrast, lowering ambient oxygen to 3% enabled cells expressing 5LO to continue to proliferate (Figure 4B). In addition, 5LO-mediated growth arrest and SA-β-gal accumulation were rescued by the antioxidant NAC or by AA861 in 20% oxygen (data not shown and Figure 4C). Therefore, 5LO pathway generates ROS, O_2^- and H_2O_2 in particular, which in turn promotes stasis.

To test whether 5LO-induced stasis is bypassed by constitutive expression of catalytically active human telomerase (hTERT), we coinfected hTERT-expressing human fibroblasts along with the respective 5LO constructs. In the case of 5LO, no differences in the inhibition of cell proliferation (Supplementary Figure 3) or SA-β-gal accumulation (data not shown) were observed. Thus, the induction of stasis by 5LO-linked cascade is hTERT independent.

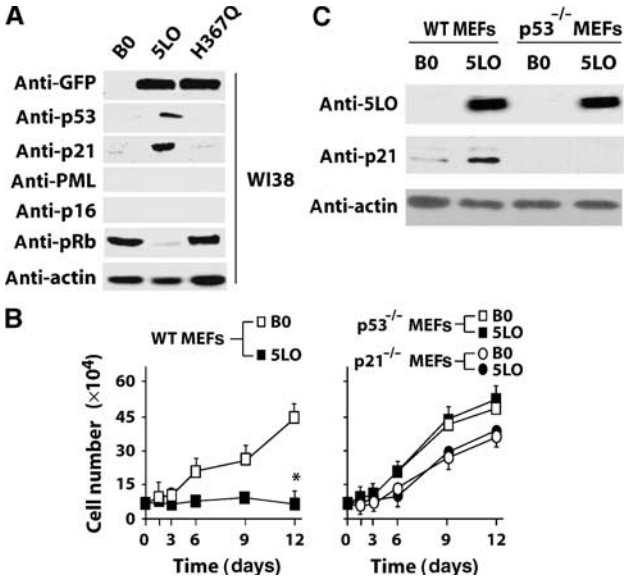

Figure 5 5LO induces stasis engaging p53/p21 pathway. (**A**) Western blot analysis of GFP, p53, p21, PML, p16, pRb and actin in WI38 cells containing an empty vector (B0), GFP-tagged 5LO or its mutant H367Q. (**B**) Growth curves of $p53^{-/-}$ or $p21^{-/-}$ MEFs infected with B0 or 5LO vectors. $^*P \leqslant 0.05$ versus B0, paired *t*-test, $n = 3$. (**C**) Immunoblotting of 5LO and p21 in both wild-type and $p53^{-/-}$ MEFs infected with B0 or 5LO vectors. Expression of actin was used as an internal control.

5LO elicits stasis via p53-dependent mechanism

The p53/p21 pathway contributes to stasis induced by oncogenic *ras* (Pearson *et al*, 2000). 5LO-expressing WI38 cells showed an accumulation of p53 (four- to five-fold) and p21 (five- to six-fold), a decrease of pRb phosphorylation and they did not show any difference of PML and p16 protein levels in comparison to controls (Figure 5A). To determine the role of p53 and p21 in 5LO-induced arrest, we infected MEFs derived from *p53*- ($p53^{-/-}$) or *p21*-deficient ($p21^{-/-}$) mice with pBabe-5LO vectors. 5LO overexpression reduced cell proliferation in MEFs, but it did not induce growth arrest in both $p53^{-/-}$ and $p21^{-/-}$ MEFs (Figure 5B). Therefore, p53 and p21 are essential for 5LO-induced growth arrest. Expression of p21 is regulated by p53-dependent or -independent mechanisms as well as protein degradation (Fotedar *et al*, 2004). To investigate the mechanism by which 5LO increases p21 expression, 5LO-expressing wild-type and $p53^{-/-}$ MEFs were then analyzed by immunoblotting. 5LO upregulated p21 in wild-type MEFs but not in $p53^{-/-}$ MEFs (Figure 5C), indicating that p53 is crucial for 5LO-mediated p21 upregulation.

ROS production by 5LO-linked cascade regulates p53 phosphorylation and transactivation

To clarify the mechanism by which 5LO activated p53-dependent pathway, we first examined the expression of p53 and p21 proteins in Ha-RasV12-expressing wild-type and $5LO^{-/-}$ MEFs. Ha-RasV12 induced comparable amounts of p53 as well as p16 proteins in both cell types (Figure 6A), and these proteins were still induced in the presence of NAC or AA861 (data not shown). However, a slight, but reproducible, reduction of p21 upregulation occurred in $5LO^{-/-}$ MEFs (8- and 4.5-fold increase in wild-type and $5LO^{-/-}$ MEFs, respectively) (Figure 6A) or in wild-type MEFs treated with NAC

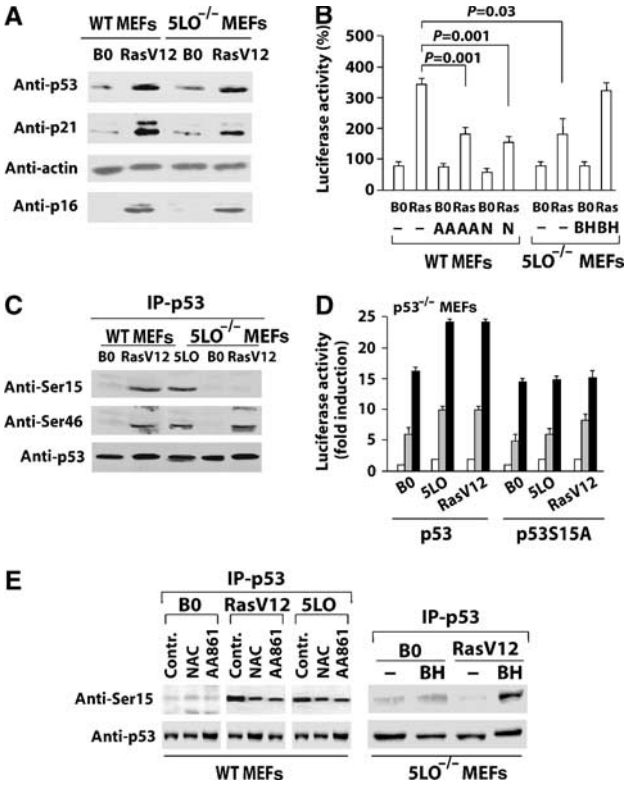

Figure 6 5LO promotes p53 phosphorylation. (**A**) Western blot analysis of p21, p53, actin and p16 upon infection of wild-type and $5LO^{-/-}$ MEFs with control (B0) or Ha-RasV12 vectors. (**B**) The luciferase reporter gene plasmid p21-luc was transfected into wild-type and $5LO^{-/-}$ MEFs infected with B0 or Ha-RasV12 and cultured in the absence or presence of 1 μM AA861 (AA), 2 mM NAC (N) or 10 μM t-BTH (BH). At 24 h after transfection, the luciferase activity was measured. The activity in B0-infected wild-type MEFs is set at 100%. *P*-values are also indicated, paired *t*-test, $n = 3$. (**C**) Wild-type and $5LO^{-/-}$ MEFs were infected with control (B0), Ha-RasV12 or 5LO. Cell lysates were prepared when Ha-RasV12- or 5LO-infected culture was terminally arrested, immunoprecipitated with anti-p53 antibody and analyzed by Western blot using anti-p53-phosphoSer15 and Ser46 antibodies. (**D**) Luciferase activity of p21-luc in $p53^{-/-}$ MEFs untransfected (□) or transfected with 50 pg (▒) or 100 pg (■) of wild-type p53 or p53S15A constructs in the presence of control (B0) or Ha-RasV12- or 5LO-expressing vectors. Values are normalized by cotransfected β-gal. (**E**) MEFs were infected with Ha-RasV12, 5LO or control (B0) and cultured with or without NAC (2 mM) or AA861 (1 μM). Cell lysates were prepared as described in the legend to panel C and protein levels of p53 and phosphoSer15 were detected by Western blotting (left). $5LO^{-/-}$ MEFs expressing control (B0) or Ha-RasV12 were untreated or treated with 10 μM t-BTH as described in the legend to Figure 2C. Protein levels of p53 and phosphoSer15 were detected by Western blotting.

or AA861 (data not shown). Thus, 5LO seems to regulate p53 activity rather than stability. To confirm this, we transfected Ha-RasV12-infected wild-type and $5LO^{-/-}$ MEFs with a luciferase reporter vector driven by the p21 promoter (p21-luc). In $5LO^{-/-}$ MEFs, Ha-RasV12-induced p53 transactivation was reduced compared to wild-type MEFs and the addition of t-BTH (10 μM) recovered Ha-RasV12-induced p53 transcriptional activity (Figure 6B). In wild-type MEFs, the enhancement of luciferase activity by Ha-RasV12 was significantly lower after treatment with either AA861 or NAC (Figure 6B). Thus, inhibition of 5LO cascade as well as addition of antioxidant NAC reduced oncogenic *ras*-induced p53 transcriptional activity.

p53 is activated by a variety of signals, some of which produce specific p53 post-translational modifications (Appella and Anderson, 2001). In particular, p53 phosphorylation accumulates during cellular senescence (Ferbeyre *et al*, 2000; Pearson *et al*, 2000). We compared the status of p53 phosphorylation during Ha-RasV12-induced stasis in wild-type and $5LO^{-/-}$ MEFs, as well as in 5LO-overexpressing cells. The phosphorylation of immunoprecipitated p53 was assessed using antibodies specific for phosphorylated Ser9, 15, 46 and 392. Ha-RasV12 increased p53 phosphorylation at Ser46 in wild-type or $5LO^{-/-}$ MEFs (Figure 6C). Ser46 phosphorylation was also increased in 5LO-expressing MEFs (Figure 6C). By contrast, Ser15 phosphorylation was observed in either Ha-RasV12- or 5LO-expressing cells, and it was dramatically reduced in $5LO^{-/-}$ MEFs (Figure 6C). Moreover, we could not detect any change in phosphorylation at Ser9 and 392 induced by Ha-RasV12 or 5LO expression (data not shown).

Further, we investigated whether Ser15 phosphorylation is relevant for p53 activation induced by 5LO. Transient transfection of wild-type p53 in $p53^{-/-}$ MEFs activated the p21-luc in a dose-dependent manner (Figure 6D). p53 mutant defective for phosphorylation at Ser15 (p53S15A) yielded similar levels of promoter activation. Coexpression of 5LO or Ha-RasV12 increased the transcriptional activity of wild-type p53 but not that of p53S15A (Figure 6D), indicating that Ser15 phosphorylation is required for p53 activation induced by 5LO and Ha-RasV12. To examine whether Ser15 phosphorylation is dependent on 5LO-mediated ROS induction, we treated Ha-RasV12- or 5LO-expressing MEFs with NAC or AA861. Both treatments inhibited Ser15 phosphorylation (Figure 6E, left panel). Moreover, this phosphorylation was recovered in $5LO^{-/-}$ MEFs expressing Ha-RasV12 and treated with t-BTH (Figure 6E, right panel). Thus, 5LO-induced ROS production is important for a full p53 phosphorylation and activity during stasis.

5LO regulates the in vitro lifespan of human and murine fibroblasts

Human lung fibroblasts undergo oxidative crises during their culture history so that their growth arrest often represents a combination of replicative senescence and stasis (Atamna *et al*, 2000; Forsyth *et al*, 2003). To test the involvement of 5LO in mediating the oxidative crisis in human fibroblasts, WI38 cells were serially passaged until they entered a senescence-like growth arrest, and protein and conditioned medium samples were collected at several stages. Senescent cells had higher 5LO protein levels than young fibroblasts (Figure 7A). This increase was readily associated with accumulation of p53 and p21, p53 phosphorylation at Ser15 and pRb hypophosphorylation (Figure 7A). In addition, a significant increase in 5LO product formation was observed in conditioned media of late-passage and senescent cells (Figure 7B). 5LO upregulation is also shown in IMR-90 and LF1 senescence fibroblasts, whereas it did not occur in confluent WI38 cells (data not shown). ROS production increased during culture history, and incubation with AA861 reduced this increase in a dose-dependent manner (Figure 7C). Accordingly, AA861 and NAC strongly reduced Ser15 phosphorylation of p53 induced during cell culture history (Figure 7D). AA861 also extended the *in vitro* lifespan of WI38 cells in a dose-dependent manner (Figure 7E).

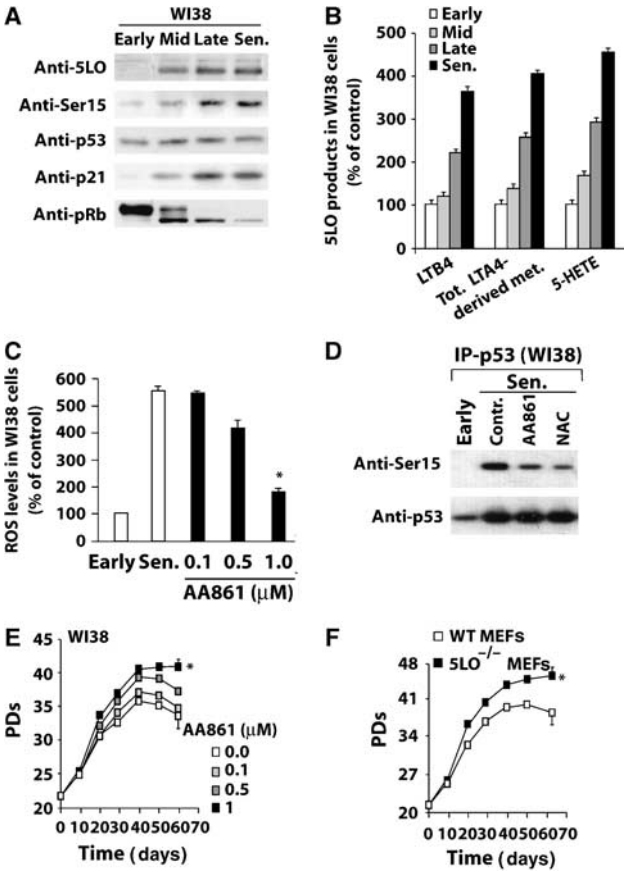

Figure 7 5LO controls cellular lifespan of primary fibroblasts. (**A**) WI38 fibroblasts were serially subcultured from early passage until they acquired the senescent phenotype. Protein extracts were prepared at the indicated times: early passage, p14; midpassage, p28; late passage, p37; senescence, p44. Representative Western blots of 5LO, p53, Ser15 p53, p21 and pRb from three independent experiments are shown. (**B**) 5LO metabolites in conditioned media of early passage, midpassage, late passage and senescence cells were measured as described in Materials and methods. (**C**) DCF fluorescence intensity of WI38 fibroblasts subcultured from early passage (p14) until senescence (p44) in the presence of indicated concentrations of AA861. (**D**) Cell lysates were prepared at the early passage and senescence, immunoprecipitated with anti-p53 antibody and analyzed by Western blot using anti-p53-phosphoSer15 antibodies. (**E, F**) Growth curves of WI38 cells incubated with different concentrations of AA861 (E) or wild-type and $5LO^{-/-}$ MEFs (F). The number of population doublings (PDs) was determined over the indicated period of time. $^{*}P \leqslant 0.05$ versus controls, ANOVA, $n = 3$.

On the other hand, replicative senescence of MEFs is a primary consequence of severe oxidative stress, which causes extensive DNA damage (Parrinello *et al*, 2003). Increased 5LO expression and activity are also shown in senescence MEFs (data not shown) and $5LO^{-/-}$ MEFs showed a significant increase of *in vitro* lifespan compared to wild-type MEFs (Figure 7F). These data support the idea that 5LO may be a key component in mediating oxidative crisis in human and murine fibroblasts that, in turn, can promote p53 phosphorylation and stasis.

Discussion

In the present study, we provide the first evidence showing the involvement of 5LO in mediating the oxidative crisis in both human fibroblasts and MEFs which determines stasis. There are a variety of systems whose function is to restrict the proliferation of premalignant or malignant cells. Telomere-based replicative senescence prevents premalignant cells from accumulating sufficient mutations to become cancerous. The induction of growth arrest by stasis (i.e. stress or aberrant signaling-induced senescence) represents an additional mechanism of preventing the proliferation of aberrant cells (Drayton and Peters, 2002). In response to inadequate culture conditions or excessive mitogenic stimuli, cells respond with a program (i.e. stasis) that induces an irreversible growth arrest and is indistinguishable from replicative senescence in terms of morphological and molecular markers (Serrano *et al*, 1997; Schmitt, 2003). Several lines of evidence suggest that ROS production is involved in both senescence pathways (stasis and replicative senescence) (Serrano *et al*, 1997; Lee *et al*, 1999). In particular, it appears that ROS is involved in the cellular commitment to senescence induction and in the transition from reversible growth arrest to a permanent one (Macip *et al*, 2003). However, the sources of ROS during cellular senescence are not completely known. Two different mechanisms that control redox signaling were recently implicated: (i) generation of ROS secondary to mitochondrial disruption and (ii) activation of cellular NADPH oxidase (Haendeler *et al*, 2004). There are other sources of cellular ROS, including the signaling of arachidonic acid, which represents a paradigm for the use of oxygen in the transmission of information (Soberman and Christmas, 2003). Here, we have focused on enzymes that control the multiple signaling pathways of arachidonic acid with the intent to identify those implicated in cellular senescence. We identified the candidate 5LO, cPLA2 and COX2 as genes upregulated during oncogenic *ras*-induced stasis (Figure 1). However, several observations suggest that the 5LO pathway of arachidonic acid metabolism is the main signal involved in ROS generation and stasis. First, the onset of stasis is accompanied by a striking increase in the production of 5-HETE, LTB4 and other LTA4-derived metabolites. Second, the effects of specific inhibitors of cPLA2 and 5LO showed that activation of cPLA2 and metabolism of the synthesized arachidonic acid by 5LO were essential for the generation of ROS and SA-β-gal accumulation by oncogenic *ras* (Figure 2). Consistently, ROS production and growth arrest following Ha-RasV12 expression can be prevented using MEFs deficient in 5LO (Figure 3). Third, the role of 5LO in mediating ROS generation was further confirmed by the significant increase of ROS levels elicited by overexpression of a catalytically active 5LO in the cells (Figure 4). Consistent with that role, the ability of 5LO to increase ROS levels is essential for the 5LO phenotype because 5LO-expressing cells grown in the presence of either a peroxide-scavenging antioxidant or low oxygen are rescued from stasis (Figure 4B and C). By contrast, 5LO-mediated stasis, like oncogenic *ras* (Wei *et al*, 1999), is not rescued by overexpression of hTERT.

Increasing evidence supports a signaling link between 5LO pathway and ROS generation. For example, the activity of 5LO is required for ROS production by CD28 stimulation in T lymphocytes (Los *et al*, 1995). Also, an action of LTB4 through an autocrine stimulatory loop was shown to be crucial for ROS generation in response to TNF-á in fibroblasts (Woo *et al*, 2000). Consistent with that report, we observed a significantly enhanced extracellular secretion of LTB4 in

response to oncogenic *ras* (Figure 1C), and ZK-158252, a specific LTB4 receptor (BLTR) antagonist, markedly inhibited Ha-RasV12-induced ROS (our unpublished data). Thus, it may be possible that 5LO is required for oncogenic *ras*-induced ROS generation and that LTB4 acts via an autocrine loop functioning as a feedback mechanism amplifying the ROS generation and, in turn, stasis. However, we cannot exclude the possibility that other 5LO products such as 5(S)-HETE, 5-oxo-HETE, the cysteinyl-LTs or lipoxins may influence stasis. The roles of specific LO metabolites during stasis are currently under investigation.

It is interesting that COX2 overexpression did not induce stasis. Both 5LO and COX2 are oxidizing enzymes forming hydroperoxy fatty acids, and lipid peroxides may be involved in the generation of ROS and stasis. However, we provide direct evidence for the chemical identity of the oxidizing species in the 5LO-expressing cells. We found that 5LO-expressing cells generate more than one reactive species (Figure 4A), whereas COX2 overexpression did not induce oxygen radicals in our systems (data not shown). This is consistent with a previous report showing that oxygen radicals seem to be not directly involved in COX2 catalytic cycle (Jiang *et al*, 2004), and suggests that several reactive species, including ROS, may contribute to the induction of stasis.

Given the known ability of ROS to induce DNA damage, it is conceivable that in the context of a normal cell, oxidative crisis resulted in oxidative modifications of DNA and the subsequent upregulation of cell cycle inhibitors, such as p53 and p21 (Serrano *et al*, 1997). Consistently, we found that 5LO increased p53 and p21 protein levels and that p53 is crucial for 5LO-mediated stasis (Figure 5). p53 phosphorylation accumulates during stasis (Ferbeyre *et al*, 2000; Pearson *et al*, 2000) and this is important for the p53 transcriptional activity (Appella and Anderson, 2001). We found that ROS produced by 5LO increases p53 phosphorylation on serine 15 (Figure 6), which is a key site for p53 regulation (Ferbeyre *et al*, 2000; Pearson *et al*, 2000). This effect may be indirect and involve p38 MAPK since this kinase is activated by 5LO metabolites (Ding *et al*, 2003) as well as oncogenic *ras* (Wang *et al*, 2002), and directly phosphorylates p53 (Bulavin *et al*, 1999). The role of p38 MAPK within this context is being investigated.

To support our findings, we also observed that 5LO is involved in human and murine fibroblasts undergoing oxidative crises during their culture history (Figure 7), a program that represents a combination of replicative senescence and stasis (Atamna *et al*, 2000; Forsyth *et al*, 2003; Parrinello *et al*, 2003), but has little to do with ageing (Drayton and Peters, 2002). In fact, 5LO gene knockout experiments in mice indicate no obvious problems in development or life expectance (Chen *et al*, 1994). However, our results suggest that 5LO modulates oxidative events, and its role may become evident only under physiological or pathological stress.

Like oncogenic *ras*, it is known that 5LO has mitogenic activity promoting the proliferation of different cell types (Soberman and Christmas, 2003). 5LO overexpression and abnormal production of leukotrienes are also involved in the pathophysiology of cancer (Hong *et al*, 1999). Therefore, 5LO-induced growth arrest may be another antitumorigenesis mechanism similar to Ras-induced stasis. We have previously shown that 5LO is able to inhibit apoptosis in cancer cell lines (Catalano *et al*, 2004). In the light of the results we present here, we argue that 5LO is part of a safeguard mechanism against tumorigenesis in normal cells. However, in cancerous cells, when all the safeguard checkpoints had been overcome, 5LO activity turns out to give a proliferative advantage to the transformed cells, resulting from inhibition of cell death.

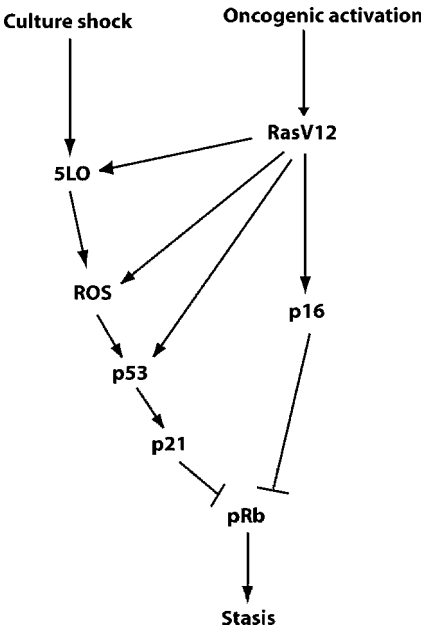

Figure 8 Summary of stasis program involving 5LO-linked cascade in primary fibroblasts. For simplicity, only RasV12-mediated oncogenic activation and 'culture shock' are shown, although a number of other effectors and/or stimuli are known to be capable of inducing stasis.

Lee *et al* (1999) suggest that one potential mediator of Ras-induced ROS generation is ceramide, a lipid linked to the senescent phenotype. Recently, it was shown that ceramide binds and activates cPLA2 increasing arachidonic acid release (Huwiler *et al*, 2001). Thus, it is possible that ceramide participates upstream of 5LO pathway in mediating the Ras response.

In conclusion, our results suggest that constitutive activation of 5LO pathway by oncogenic activation (i.e. Ha-RasV12) or 'culture shock' leads to an increase of ROS that promotes stasis via the p53/p21-dependent pathway (Figure 8). Given that Ha-RasV12 induction of p53 and p16 is not dependent on 5LO activity (see Figure 6), it would appear that an oncogenic *ras* target other than 5LO participates to induce p53 and p16. Our results also show that NADPH oxidase inhibitors produce as great a reduction in ROS levels and stasis as 5LO inhibitors. Thus, it may be sufficient to block either pathway in order to prevent the Ras-induced response. The induction of p53 by Ha-RasV12 also occurs in the 5LO-deficient MEFs, and there is only an approximately 50% reduction in the amount of p21 induced (indicating that p53 may be active in spite of not being phosphorylated on Ser15). Thus, it appears that there are a variety of pathways contributing to the mechanism by which growth arrest is achieved, and it is only when all are active that the response is obtained. It is not clear whether 5LO is directly (by production of pro-oxidant 5LO metabolites as end products) or indirectly (by production of 5LO metabolites as intermediates in a pathway) responsible for ROS generation during stasis. However, our findings uncover

novel functions of 5LO and indicate that the products of the 5LO pathway can function as amplifiers of oxidative stress involved in cellular senescence.

Materials and methods

Cells and culture conditions

Normal human fibroblasts IMR-90 (ATCC CCL-186), LF1 (ATCC CCL-153) and WI38 (ATCC CCL-75) were cultured in Ham's F-10 medium supplemented with 15% fetal bovine serum (FBS), nonessential amino acids and sodium pyruvate (all from HyClone, Rome, Italy). $5LO^{-/-}$ MEFs were prepared from $5LO^{-/-}$ mice, whereas $p21^{-/-}$ MEFs were prepared from embryos derived from crosses between heterozygous mice (Jackson, Bar Harbor, ME). MEFs were cultured in Dulbecco's modified Eagle's medium supplemented with 10% FBS and penicillin–streptomycin (50 U/ml). For H_2O_2 treatment (Gorbunova *et al*, 2002), we added to the culture medium 250 μM H_2O_2 for 2 h. Then, cells were washed once with phosphate-buffered saline (PBS) and a fresh culture medium was added. For infected cells (Ferbeyre *et al*, 2000), we selected with 1 μg/ml puromycin for 4 days. The day when drug selection was completed (4 days after infection or H_2O_2 treatment) was defined as day 0.

Chemicals and vectors

MK886, AA861, indometacin, ATK and ETYA were purchased from Cayman Chemical (Milan, Italy). DCF, DPI and NAC were from Sigma (Milan, Italy). All other chemicals were from standard sources and were molecular biology grade or higher. The retroviral Babe-puro-Ha-RasV12 and pBabe empty (B0) vectors were kindly provided by Dr GJ Clark (National Cancer Institute, MD). The plasmids coding wild-type p53 and p53S15A were described previously (D'Orazi *et al*, 2002), and were provided by Dr S Soddu (Regina Elena Cancer Institute, Rome, Italy). The cDNA of wild-type 5LO-GFP fusion protein or catalytically inactive 5LO mutant, H367Q-GFP fusion protein was previously reported (Romano *et al*, 2001; Catalano *et al*, 2004), and was subcloned into Babe-puro. DNA sequencing was performed to verify the correct insertion with a MegaBACE DNA analysis system by using a DYEnamic ET Dye Terminator Cycle sequencing kit (Amersham Corp., Milan, Italy). Details of the construct are available upon request. Retroviral stocks were generated by transient transfection of packaging cell line (PT67, Clontech, Palo Alto, CA) and stored at −80°C until use. Infection of cells with retroviral constructs, and culturing of transduced cells were performed by standard procedures (Serrano *et al*, 1997; Bischof *et al*, 2002).

Reporter assays

Infected WI38 fibroblasts ($5–8 \times 10^3/cm^2$ on 35 mm dishes) were transfected with 500 ng p21-Luciferase (p21-Luc) reporter plasmid (Catalano *et al*, 2004) and 0.1 μg pCMV-β-gal reporters using LipofectAMINE 2000 (Invitrogen, Milan, Italy). β-Galactosidase and luciferase activities were measured using Galacto-Light Plus™ (Tropix Inc., Bedford, MA) and Luciferase Assay Systems (Promega, Milan, Italy) according to the suppliers' instructions and as reported earlier (Catalano *et al*, 2004). Luciferase activity was then normalized with β-galactosidase activity.

Senescence analysis

Senescence was assessed using several assays. The growth curves were performed as described (Bischof *et al*, 2002). Cells were plated in triplicate at 2×10^4 per well in 12-well plates. Relative cell numbers were estimated at various time points using a crystal violet incorporation assay, and the number of PDs (n) was calculated using the following equation:

$$n = (\log_{10} F - \log_{10} I) \times 3.32$$

where F is the number of cells at the end of one passage and I is the number of cells that were seeded at the beginning of one passage. Thymidine incorporation assay and SA-β-gal staining were performed as described (Gorbunova *et al*, 2002). Cells were subcultured on coverslips. When 70–80% confluent at $2 \times 10^4/cm^2$, [^{3}H]thymidine (10 μCi/ml) was added to the cells for an additional 36 h, fixed and subjected to autoradiography, and the percentage of cells incorporating [^{3}H]thymidine was determined. These cells were also costained for SA-β-Gal. Cells were counted under the microscope, and a minimum of 500 cells were counted for each coverslip. The percent of SA-β-gal-positive cells from the total number of cells was calculated.

Real-time RT–PCR

Cells were collected after indicated times and washed with PBS. Total RNA was extracted with the RNeasy minikit from Qiagen (Milan, Italy). Total RNA (50 ng/μl) from different treatments was reverse transcribed with the TaqMan reverse transcription kit (PE Applied Biosystem, Milan, Italy). The cDNA was then subjected to real-time reverse transcription (RT)–PCR with SYBR Green PCR core reagents (Finnzymes, Keilaranta, Finland). The PCR were carried out in a Chromo4 sequence detector (Celbio, Milan, Italy). The primer sequences of all 5LO pathway constituents were determined by Laboratory Tools software analysis of Stratagene (Milan, Italy). Details of sequences and thermal cycle conditions are available upon request. The amplicons of genes were between 250 and 300 bp. Data were acquired and analyzed with the sequence detector Chromo4 software.

Protein expression

Immunoprecipitation and Western blot analysis were performed from whole cell lysates as previously described (Catalano *et al*, 2004). Antibodies against 5LO (Cayman Chemical, Milan, Italy), p53 (DO1, Santa Cruz, Milan, Italy), Ser15 (16G8), Ser46 p53 (Cell Signaling Tec., Milan, Italy), p21 (Ab1), RasV12 (OP38, Calbiochem, Milan, Italy), p16 (DCS-50, Novocastra), pRb, cPLA, COX2 (all by Cell Signaling Tec., Milan, Italy) and PML (PGM3, Santa Cruz) were used as probes and detected using enhanced chemiluminescence (Amersham Corp., Milan, Italy). To determine expression of the catalytically inactive H367Q mutant, Western blot analysis was carried out using anti-GFP monoclonal antibody (Calbiochem, Milan, Italy). As loading control, the blots were reprobed with an anti-β-actin antibody.

Measurements of 5LO products

Mono-HETEs released into cell conditioned media were determined using solid phase extraction and reversed-phase (RP) high-performance liquid chromatography (HPLC) procedures as described previously (Catalano *et al*, 2004). To determine LT isomers and metabolites, we also utilized RP-HPLC procedures described by Hosni *et al* (1991), with detection at 270 nm. Prostaglandins E1 (PGE1) and B2 (PGB2), 5-HETE, 15*S*-hydroxyeicosatrienoic acid (15-HETrE), LTB4 and other arachidonic acid metabolites used as standards for HPLC were from Cayman (Milan, Italy). Methanol and acetonitrile were of HPLC grade. Other reagents were of analytical grade or better. 5LO product formation is expressed as nanogram of 5LO products per milligram of protein. 20-COOH-LTB4 is not detected by RP-HPLC.

Measurement of ROS, superoxide, hydrogen peroxide, nitrite anion and 8-isoprostane generation

For measurement of ROS production, cells were incubated with 5 μg/ml of DCF for 30 min at 37°C, washed with PBS, trypsinized and collected in 1 ml of PBS, followed by fluorescence-activated cell sorter (FACS; Beckton Dickson FACScan) using Cell Quest 3.2 software (Beckton Dickson, Milan, Italy) for analysis. Values of mean green fluorescence intensity were used to plot graphs. Superoxide anion (O_2^-) generation was determined by lucigenin (25 μM, final concentration) as previously described (Altmann *et al*, 2004). The chemiluminescence was recorded using a Micro Luminat Plus LB 96V (Berthold, Bad Wildbad, Germany) at intervals of 6 s (two cycles) in a total detection time of 3 min. The detected chemiluminescence was summarized over two intervals and plotted versus blank values. H_2O_2 concentration was determined as previously described (Moreno, 2003). Briefly, 2,6-dichlorophenolindophenol (DCPIP, 40 μM) was reduced by ascorbic acid, which attenuated the blue color. H_2O_2 in samples in the presence of a few microliters of horseradish peroxidase increased the absorbance (610 nm) owing to the reoxidation of DCPIP. Control reactions were performed by adding catalase. The 8-isoprostane was measured using the corresponding ELISA kit from Cayman Chemicals (Milan, Italy), and nitrite (NO_2^-) accumulation in the cell-free supernatant, as an indicator of NO production, was measured using the Griess reagent as described elsewhere (Martinez *et al*, 2000). The production of NO_2^- was measured from

a sodium nitrite standard curve freshly prepared in culture medium and expressed in nmol. The detection limit was 1 μM.

Annexin and propidium iodide fluorescent staining

Annexin and PI fluorescent staining was carried out as described previously (Rippo *et al*, 2004). Cells positively stained with annexin and not PI were considered apoptotic, and cells negative for the two dyes were considered live cells.

Statistical analysis

All values were expressed as mean ± s.e.m. Comparison of results between different groups was performed by one-way analysis of variance and paired *t*-test using StatView 5.0 (NET Engineering, Pavia, Italy). A *P*-value $\leqslant 0.05$ was considered to be statistically significant.

Supplementary data

Supplementary data are available at *The EMBO Journal* Online.

Acknowledgements

We acknowledge Dr Geoffrey J Clark (National Cancer Institute, National Institutes of Health, MD) for providing pBabe and pBabe HaRasV12 vectors, Dr S Soddu (Regina Elena Cancer Institute, Rome, Italy) for p53 constructs and Dr PierGiuseppe Pelicci (IFOM-FIRC Institute, Milan, Italy) for discussions. This work has been funded by AIRC, FIRC, MIUR and Ministero della Sanità grants to AP. AC was supported by a fellowship from FIRC.

References

Altmann A, Poeckel D, Fischer L, Schubert-Zsilavecz M, Steinhilber D, Werz O (2004) Coupling of boswellic acid-induced Ca^{2+} mobilisation and MAPK activation to lipid metabolism and peroxide formation in human leucocytes. *Br J Pharmacol* **141:** 223–232

Appella E, Anderson CW (2001) Post-translational modifications and activation of p53 by genotoxic stresses. *Eur J Biochem* **268:** 2764–2772

Atamna H, Paler-Martinez A, Ames BN (2000) *N*-t-butyl hydroxylamine, a hydrolysis product of alpha-phenyl-*N*-t-butyl nitrone, is more potent in delaying senescence in human lung fibroblasts. *J Biol Chem* **275:** 6741–6748

Bischof O, Kirsh O, Pearson M, Itahana K, Pelicci PG, Dejean A (2002) Deconstructing PML-induced premature senescence. *EMBO J* **21:** 3358–3369

Bringold F, Serrano M (2000) Tumor suppressors and oncogenes in cellular senescence. *Exp Gerontol* **35:** 317–329

Bulavin DV, Saito S, Hollander MC, Sakaguchi K, Anderson CW, Appella E, Fornace AJ (1999) Phosphorylation of human p53 by p38 kinase coordinates N-terminal phosphorylation and apoptosis in response to UV radiation. *EMBO J* **18:** 6845–6854

Campisi J (2001) Cellular senescence as a tumor-suppressor mechanism. *Trends Cell Biol* **11:** 27–31

Catalano A, Caprari P, Soddu S, Procopio A, Romano M (2004) 5-Lipoxygenase antagonizes genotoxic stress-induced apoptotis by perturbing p53 nuclear trafficking. *FASEB J* **18:** 1740–1742

Chen XS, Sheller JR, Johnson EN, Funk CD (1994) Role of leukotrienes revealed by targeted disruption of the 5-lipoxygenase gene. *Nature* **372:** 179–182

Ding XZ, Tong WG, Adrian TE (2003) Multiple signal pathways are involved in the mitogenic effect of 5(S)-HETE in human pancreatic cancer. *Oncology* **65:** 285–294

D'Orazi G, Cecchinelli B, Bruno T, Manni I, Higashimoto Y, Saito S, Gostissa M, Coen S, Marchetti A, Del Sal G, Piaggio G, Fanciulli M, Appella E, Soddu S (2002) Homeodomain-interacting protein kinase-2 phosphorylates p53 at Ser 46 and mediates apoptosis. *Nat Cell Biol* **4:** 11–19

Drayton S, Peters G (2002) Immortalization and transformation revisited. *Curr Opin Genet Dev* **12:** 98–104

Ferbeyre G, de Stanchina E, Querido E, Baptiste N, Prives C, Lowe SW (2000) PML is induced by oncogenic ras and promotes premature senescence. *Genes Dev* **14:** 2015–2027

Forsyth NR, Evans AP, Shay JW, Wright WE (2003) Developmental differences in the immortalization of lung fibroblasts by telomerase. *Aging Cell* **2:** 235–243

Fotedar R, Bendjennat M, Fotedar A (2004) Role of p21WAF1 in the cellular response to UV. *Cell Cycle* **3:** 134–137

Gorbunova V, Seluanov A, Pereira-Smith OM (2002) Expression of human telomerase (hTERT) does not prevent stress-induced senescence in normal human fibroblasts but protects the cells from stress-induced apoptosis and necrosis. *J Biol Chem* **277:** 38540–38549

Haendeler J, Hoffmann J, Diehl JF, Vasa M, Spyridopoulos I, Zeiher AM, Dimmeler S (2004) Antioxidants inhibit nuclear export of telomerase reverse transcriptase and delay replicative senescence of endothelial cells. *Circ Res* **94:** 768–775

Hong SH, Avis I, Vos MD, Martinez A, Treston AM, Mulshine JL (1999) Relationship of arachidonic acid metabolizing enzyme expression in epithelial cancer cell lines to the growth effect of selective biochemical inhibitors. *Cancer Res* **59:** 2223–2228

Hosni R, Chabannes B, Pacheco Y, Moliere P, Grosclaude M, Perrin Fayolle M, Lagarde M (1991) Leukotriene B4 levels from stimulated neutrophils from healthy and allergic subjects: effect of platelets and exogenous arachidonic acid. *Eur J Clin Invest* **21:** 631–637

Huwiler A, Johansen B, Skarstad A, Pfeilschifter J (2001) Ceramide binds to the CaLB domain of cytosolic phospholipase A2 and facilitates its membrane docking and arachidonic acid release. *FASEB J* **15:** 7–9

Jiang J, Borisenko GG, Osipov A, Martin I, Chen R, Shvedova AA, Sorokin A, Tyurina YY, Potapovich A, Tyurin VA, Graham SH, Kagan VE (2004) Arachidonic acid-induced carbon-centered radicals and phospholipid peroxidation in cyclo-oxygenase-2-transfected PC12 cells. *J Neurochem* **90:** 1036–1049

Lee AC, Fenster BE, Ito H, Takeda K, Bae NS, Hirai T, Yu ZX, Ferrans VJ, Howard BH, Finkel T (1999) Ras proteins induce senescence by altering the intracellular levels of reactive oxygen species. *J Biol Chem* **274:** 936–940

Lewis RA, Austen KF, Soberman RJ (1990) Leukotrienes and other products of the 5-lipoxygenase pathway. Biochemistry and relation to pathobiology in human diseases. *N Engl J Med* **323:** 645–655

Los M, Schenk H, Hexel K, Baeuerle PA, Droge W, Schulze-Osthoff K (1995) IL-2 gene expression and NF-κB activation through CD28 requires reactive oxygen production by 5-lipoxygenase. *EMBO J* **14:** 3731

Lundberg AS, Hahn WC, Gupta P, Weinberg RA (2000) Genes involved in senescence and immortalization. *Curr Opin Cell Biol* **12:** 705–709

Macip S, Igarashi M, Berggren P, Yu J, Lee SW, Aaronson SA (2003) Influence of induced reactive oxygen species in p53-mediated cell fate decisions. *Mol Cell Biol* **23:** 8576–8585

Martinez J, Sanchez T, Moreno JJ (2000) Regulation of prostaglandin E2 production by the superoxide radical and nitric oxide in mouse peritoneal macrophages. *Free Radic Res* **32:** 303–311

Mathon NF, Lloyd AC (2001) Cell senescence and cancer. *Nat Rev Cancer* **1:** 203–213

Moreno JJ (2003) Effect of olive oil minor components on oxidative stress and arachidonic acid mobilization and metabolism by macrophages RAW 264.7. *Free Radic Biol Med* **35:** 1073–1081

Parrinello S, Samper E, Krtolica A, Goldstein J, Melov S, Campisi J (2003) Oxygen sensitivity severely limits the replicative lifespan of murine fibroblasts. *Nat Cell Biol* **5:** 741–747

Pearson M, Carbone R, Sebastiani C, Cioce M, Fagioli M, Saito S, Higashimoto Y, Appella E, Minucci S, Pandolfi PP, Pellicci PG (2000) PML regulates p53 acetylation and premature senescence induced by oncogenic Ras. *Nature* **406:** 207–210

Rippo MR, Moretti S, Vescovi S, Tomasetti M, Orecchia S, Amici G, Catalano A, Procopio A (2004) FLIP overexpression inhibits death receptor-induced apoptosis in malignant mesothelial cells. *Oncogene* **23:** 7753–7760

Romano M, Catalano A, Nutini M, D'Urbano E, Crescenzi C, Claria J, Libner R, Davi G, Procopio A (2001) 5-Lipoxygenase regulates

malignant mesothelial cell survival: involvement of vascular endothelial growth factor. *FASEB J* **15:** 2326–2336

Schmitt CA (2003) Senescence, apoptosis and therapy cutting the lifelines of cancer. *Nat Rev Cancer* **3:** 286–295

Serrano M, Blasco MA (2001) Putting the stress on senescence. *Curr Opin Cell Biol* **13:** 748–753

Serrano M, Lin AW, McCurrach ME, Beach D, Lowe SW (1997) Oncogenic ras provokes premature cell senescence associated with accumulation of p53 and p16INK4a. *Cell* **88:** 593–602

Soberman RJ, Christmas P (2003) The organization and consequences of eicosanoid signaling. *J Clin Invest* **111:** 1107–1113

Stewart SA, Weinberg RA (2000) Telomerase and human tumorigenesis. *Semin Cancer Biol* **10:** 399–406

Wang W, Chen JX, Liao R, Deng Q, Zhou JJ, Huang S, Sun P (2002) Sequential activation of the MEK-extracellular signal-regulated kinase and MKK3/6-p38 mitogen-activated protein kinase pathways mediates oncogenic ras-induced premature senescence. *Mol Cell Biol* **22:** 3389–3403

Wei S, Wei S, Sedivy JM (1999) Expression of catalytically active telomerase does not prevent premature senescence caused by overexpression of oncogenic Ha-Ras in normal human fibroblasts. *Cancer Res* **59:** 1539–1543

Woo CH, Eom YW, Yoo MH, You HJ, Han HJ, Song WK, Yoo YJ, Chun JS, Kim JH (2000) Tumor necrosis factor-á generates reactive oxygen species via a cytosolic phospholipase A2-linked cascade. *J Biol Chem* **275:** 32357–32362